

On nearfield acoustic holography

Victor Isakov¹

February 20, 2004

1 Introduction

Let Ω be a bounded domain in \mathbf{R}^n , $n = 2, 3$, with the Lipschitz boundary and connected complement $\Omega_+ = \mathbf{R}^n \setminus \bar{\Omega}$. We consider the acoustical pressure field u of frequency k satisfying the Helmholtz equation

$$\Delta u + k^2 u = 0 \quad \text{in } \Omega \quad (\text{or in } \Omega_+ = \mathbf{R}^n \setminus \bar{\Omega}). \quad (1)$$

We are interested in applications where Ω is a cabin of an aircraft or a car. Solutions to (1) in Ω_+ are assumed to satisfy the Sommerfeld radiation condition

$$\lim r^{\frac{n-1}{2}} (\partial_r u - iku)(x) = 0, \quad \text{as } r = |x| \rightarrow \infty$$

Such functions u are called radiating solutions. Pressure measurements are taken by acoustical sensors located in a domain Ω_0 inside or outside the cabin or on a surface $\Gamma_0 = \partial\Omega_0$. Our goal is to reconstruct u inside Ω , or the normal velocity $v = \partial_\nu u$ on $\Gamma = \partial\Omega$, (ν is the unit exterior normal to $\partial\Omega$). This is a mathematical model of the nearfield acoustic holography [W], [Wu].

$H_{(m)}(\Omega)$ denotes the Sobolev space of functions on Ω whose partial derivatives up to order m are square integrable over Ω , and $\|\cdot\|_{(m)}$ denotes the standard norm on this space. We set $\|\cdot\|_2 = \|\cdot\|_{(0)}$ to be the norm in the space $L^2(\Omega)$.

2 Uniqueness and stability for the inverse problem

In this section we discuss uniqueness and stability of the continuation of solutions to (1). We denote by Ω_0 a Lipschitz domain with the closure $\bar{\Omega}_0$ in Ω for the interior problem and in Ω_+ for the exterior one.

¹Department of Mathematics and Statistics, Wichita State University, Wichita, KS 67260, email: victor.isakov@wichita.edu

Lemma 2.1 *Let k^2 be distinct from a Dirichlet eigenvalue of Ω_0 . If $\Gamma_0 = \partial\Omega_0$, then $u \in H_{(1)}(\Omega)$ solving (1) is uniquely determined by its values on Γ_0 .*

To prove uniqueness, we assume that $u = 0$ on Γ_0 and we have to conclude that $u = 0$ in Ω . Since k^2 is not a Dirichlet eigenvalue, a solution to the Dirichlet problem in Ω_0 is unique, so $u = 0$ in Ω_0 . From uniqueness of the continuation from Ω_0 onto Ω , we conclude that $u = 0$ in Ω .

For the exterior problem uniqueness also holds when $\bar{\Omega} \subset \Omega_0$. Indeed, since a solution of the (exterior) Dirichlet problem with the data on $\partial\Omega_0$ is unique, then $u = 0$ on Γ_0 implies that $u = 0$ outside Ω_0 and hence, by uniqueness of the continuation, in Ω_+ .

Nonuniqueness caused by the Dirichlet eigenvalues of Ω_0 cannot be avoided, but we can modify the eigenvalues by changing the measurement surface Γ_0 . If k^2 is away from them, the Dirichlet problem in Ω_0 is stable in classical Sobolev (or Hölder) spaces. The problem of the continuation of solutions of elliptic equations (from Ω_0 onto Ω) is notoriously unstable; however, assuming that $\|u\|_2(\Omega) < M_0$, one can control exponentially growing solutions and obtain the following conditional Hölder estimate

$$\|u\|_{(k)}(\Omega_1) \leq CM^{1-\lambda}\|u\|_2^\lambda(\Omega_0),$$

where C and λ ($0 < \lambda < 1$) depend on Ω, Ω_0, k , and on the distance from $\Omega_1 \subset \Omega$ to $\partial\Omega$.

We now present a stability estimate for a special case when the domains in question are spheres in \mathbf{R}^3 : $\Omega = \{|x| < r_1\}$ and $\Omega_0 = \{|x| < r_0\}$. A solution u to the Helmholtz equation (1) in Ω admits the expansion $u(x) = \sum u_{m,n} j_n(kr) Y_{m,n}(\sigma)$, where j_n is the n -th spherical Bessel function, $r = |x|$, $\sigma = \frac{x}{r}$, and $Y_{m,n}$ are the spherical harmonics on the unit sphere. We denote by u_0 the sum of the terms with $n \leq n_1 = \frac{kr_1^2 - 3}{2}$, and by u_1 the sum of the remaining terms of the series.

Theorem 2.1 *Let u be a solution to the Helmholtz equation (1) in the ball $\Omega(r_1)$ and*

$$\|u\|_2(\Omega(r_1)) \leq M_0, \quad \|\nabla u\|_2(\Omega(r_1)) \leq M_1.$$

Then

$$\frac{r_0^3}{r^2} \|u\|_2^2(\partial\Omega(r)) \leq C_1(r)\epsilon_0^2 + C_2\epsilon_1^{2\lambda}, \quad r < r_1$$

where $\epsilon_j^2 = \|u_j\|_2^2(\partial\Omega(r_0))$, $C_1(r) = \max | \frac{j_n(kr)}{j_n(kr_0)} |^2$ over $n \leq n_1$, $C_2 = 5M^2$, $M^2 = 4M_0^2 + r_1^2 M_1^2$, and $\lambda = \frac{\ln r_1 - \ln r}{\ln r_1 - \ln r_0}$. Moreover,

$$\|u\|_2^2(\partial\Omega(r_1)) \leq C_1(r_1)\epsilon_0^2 + C_3\epsilon_2(C_4 - \ln\epsilon_2),$$

where $C_3 = \frac{1}{r_0} \max(k^2 M_0^2, M_1^2) \ln \frac{r_1}{r_0}$, $\epsilon_2 = -\frac{1}{\ln \frac{\epsilon_1}{M}}$, and $C_4 = 1 - \ln \frac{r_0^3 C_3}{5M^2}$.

This stability estimate is given in [DIVW2]. Since the number of terms included in u_1 grows, one expects an increased stability with increasing frequency. Indeed, it happens in practical computations for the nearfield acoustical holography [DIVW1], [DIVW2] for relatively small wave numbers k . However, according to classical results of Fritz John [J], stability of interior problems does not increase with frequency over the whole range of k .

In the next theorem Ω^* is an open subset of $\{x_1^2 + \dots + x_{n-1}^2 < r^2, 0 < x_n < h\}$ with the Lipschitz boundary, $\Omega_d^* = \Omega^* \cap \{d < x_n\}$, and Ω_0 is an open subset of Ω^* with $\partial\Omega \cap \{0 < x_n\} \subset \partial\Omega_0$ such that $\Gamma_0 \setminus \partial\Omega^*$ is at the distance d_0 from $\partial\Omega^*$. Let $F = \|u\|_{(1)}(\Omega_0) + \|f\|_{(0)}(\Omega)$.

Theorem 2.2 *There is a constant C not depending on d, k such that*

$$\|u\|(\Omega_d) \leq C \left(F + \frac{\|u\|_{(1)}(\Omega)^{1-\lambda} F^\lambda}{d^{2-2\lambda}(k+1)} \right)$$

for all solutions u to the Helmholtz equation (1). Here

$$\lambda = \frac{16r^2d + 3d^2}{32r^2h + 8h^2d + 2d^2h + 3d^2 + 24r^2d}.$$

This bound and its implications are obtained in [HI] by using Carleman estimates for the Helmholtz equation with constants not depending on k .

3 Representation by potentials.

In the first approach we use the single and double layer potentials

$$S_\Gamma\varphi(x) = \int_\Gamma \Phi(x, y)\varphi(y)d\Gamma(y),$$

$$D_\Gamma\varphi(x) = \int_\Gamma \partial_{\nu(y)}\Phi(x, y)\varphi(y)d\Gamma(y), \quad x \in \Omega \text{ (or } x \in \Omega_+),$$

where Φ is the free space radiating fundamental solution to (1) in \mathbf{R}^n . We recall that

$$\Phi(x, y) = \frac{1}{4\pi} \frac{e^{ik|x-y|}}{|x-y|} \quad \text{when } n = 3,$$

$$\Phi(x, y) = \frac{i}{4} H_0^{(1)}(k|x-y|) \quad \text{when } n = 2,$$

where $H_0^{(1)}$ is the Hankel function. We fix a ball B containing $\overline{\Omega}$.

Theorem 3.1 *For any solution $u \in H_{(1)}(\Omega)$ to the Helmholtz equation (1), there is a unique function $\varphi \in H_{(-\frac{1}{2})}(\Gamma)$ such that $u(x) = S_\Gamma\varphi(x)$ for all $x \in \Omega$. Moreover, for some constant C depending only on Ω , we have*

$$C^{-1}\|u\|_{(1)}(\Omega) \leq \|\varphi\|_{(-\frac{1}{2})}(\Gamma) \leq C\|u\|_{(1)}(\Omega).$$

We outline a proof of Theorem 3.1 referring for details to [DIVW2]. It is well-known, that the single layer potential S with density in $H_{(-\frac{1}{2})}(\Gamma)$ has the following properties:

$$\begin{aligned} -\Delta S_- - k^2 S_- &= 0 & \text{in } \Omega, & \quad -\Delta S_+ - k^2 S_+ = 0 & \text{in } \Omega_+, \\ S_- - S_+ &= 0, & \partial_\nu S_- - \partial_\nu S_+ &= \varphi & \text{on } \Gamma, \end{aligned} \tag{2}$$

and S_+ satisfies the radiation condition at infinity. Here S_- coincides with S on Ω and S_+ coincides with S outside Ω . Let $g \in H_{(\frac{1}{2})}(\Gamma)$ be the trace of the function u on Γ . It is well-known, that for exterior problems there is a unique radiating solution $u^+ \in H_{(1)}(B \setminus \Omega)$ to the Helmholtz equation in Ω_+ with the Dirichlet data g on Γ . In addition, the solutions u, u^+ of the interior and of the exterior Dirichlet problems in Ω with the Dirichlet data g , have their traces $\partial_\nu u, \partial_\nu u^+$ in the Sobolev space $H_{(-\frac{1}{2})}(\Gamma)$. Let $\varphi = \partial_\nu u - \partial_\nu u^+$ on Γ . We claim that Theorem 3.1 holds for this φ .

Indeed, the functions u and $S\varphi$ on Ω , and u_+ and $S_+\varphi$ on its complement, satisfy the same Helmholtz equations and the same transmission conditions at Γ (2), as well as the radiation condition at infinity. A solution of this transmission problem is unique. Hence $u = S\varphi$ in Ω .

A similar result holds for exterior problems, provided that k^2 is not a Dirichlet eigenvalue of Ω .

Theorem 3.2 *Let k^2 be distinct from a Dirichlet eigenvalue of Ω . For any radiating solution $u \in H_{(1)}(B \setminus \bar{\Omega})$ to the Helmholtz equation (1), there is a unique function φ in $H_{(-\frac{1}{2})}(\Gamma)$ such that $u(x) = S_\Gamma\varphi(x)$ for $x \in \Omega_+$. Moreover, for some constant C depending only on Ω , we have*

$$C^{-1}\|u\|_{(1)}(B \setminus \bar{\Omega}) \leq \|\varphi\|_{(-\frac{1}{2})}(\Gamma) \leq C\|u\|_{(1)}(B \setminus \bar{\Omega}).$$

Now our problem is reduced to solving the linear integral equation

$$\int_\Gamma \Phi(x, y)\varphi(y)d\Gamma(y) = u(x), \quad x \in \Gamma_0. \tag{3}$$

After determining φ in the interior problem, one can find the normal velocity from the formula

$$v(x) = \frac{1}{2}\varphi(x) + \int_\Gamma \nabla_x \Phi(x, y) \cdot \nu(x)\varphi(y)d\Gamma(y), \quad x \in \Gamma. \tag{4}$$

Lemma 3.1 *If $u \in H_{(1)}(\Omega)$ is a solution to (1), then there exist unique functions $\varphi_j \in H_{(\frac{1}{2}-j)}(\Gamma)$, ($j = 0, 1$), such that*

$$u(x) = S_\Gamma \varphi_1(x) - D_\Gamma \varphi_0(x), \quad x \in \Omega,$$

$$\frac{1}{2} \varphi_0(z) = S_\Gamma \varphi_1(z) - D_\Gamma \varphi_0(z), \quad z \in \Gamma.$$

Lemma 3.2 *Let $u \in H_{(1)}(B \setminus \Omega)$ (for any B) be a solution to (1) in Ω_+ . There exist functions $\varphi_j \in H_{(\frac{1}{2}-j)}(\Gamma)$, ($j = 0, 1$), such that*

$$u(x) = -S_\Gamma \varphi_1(x) + D_\Gamma \varphi_0(x), \quad x \in \Omega_+,$$

$$\frac{1}{2} \varphi_0(z) = -S_\Gamma \varphi_1(z) + D_\Gamma \varphi_0(z), \quad z \in \Gamma.$$

The function φ_0 is unique. If k^2 is not a Dirichlet eigenvalue of Ω , then φ_1 is unique.

Now we can write the Helmholtz-Kirchhoff system of integral equations for the interior inverse problem

$$u(x) = S_\Gamma \varphi_1(x) - D_\Gamma \varphi_0(x), \quad x \in \Gamma_0 \subset \Omega, \quad (5)$$

$$\frac{1}{2} \varphi_0(z) = S_\Gamma \varphi_1(z) - D_\Gamma \varphi_0(z), \quad z \in \Gamma, \quad (6)$$

and for the exterior problem

$$u(x) = -S_\Gamma \varphi_1(x) + D_\Gamma \varphi_0(x), \quad x \in \Gamma_0 \subset \Omega_+, \quad (7)$$

$$\frac{1}{2} \varphi_0(z) = -S_\Gamma \varphi_1(z) + D_\Gamma \varphi_0(z), \quad z \in \Gamma. \quad (8)$$

Finally, we discuss uniqueness for integral equations (3), (5)-(8).

Lemma 3.3 *(Interior problem)*

If k^2 is not a Dirichlet eigenvalue of Ω_0 , then under the conditions of Lemma 3.1, a solution $\varphi \in H_{(-\frac{1}{2})}(\Gamma)$ to the equation (3) is unique, and a solution $(\varphi_0, \varphi_1) \in H_{(\frac{1}{2})}(\Gamma) \times H_{(-\frac{1}{2})}(\Gamma)$ to the Helmholtz-Kirchhoff system (5), (6) is unique.

This follows directly from Theorem 3.1, Lemma 2.1 and Lemma 3.1.

Lemma 3.4 *(Exterior problem)*

If k^2 is not a Dirichlet eigenvalue of Ω_0 , then under the conditions of Lemma 3.2 on Γ_0 a solution $\varphi \in H_{(\frac{1}{2})}(\Gamma)$ to the equation (3) is unique and a solution $(\varphi_0, \varphi_1) \in H_{(\frac{1}{2})} \times H_{(-\frac{1}{2})}(\Gamma)$ to the Helmholtz-Kirchhoff system (7),(8) is unique.

This follows directly from Theorem 3.2, Lemma 2.2 and Lemma 3.2.

4 Approximation and completeness results

Now we discuss approximation of general solutions u by simple solutions. Our goal is to interpolate our data on Γ_0 for further solution of integral equations. This can be crucial for larger k . More importantly, we justify the very efficient HELS method of Sean Wu, see [IW], [Wu].

Theorem 4.1 *Let Ω be a bounded Lipschitz domain in \mathbf{R}^n , and let $u \in H_{(1)}(B \setminus \bar{\Omega})$ be a radiating solution to the Helmholtz equation $\Delta u + k^2 u = 0$ in Ω_+ . For any $a \in \Omega$ and any positive ε , there is a radiating solution u_ε to the Helmholtz equation outside a such that*

$$\|u - u_\varepsilon\|_{(1)}(\Omega_+ \cap B) < \varepsilon.$$

This result follows from the Runge property and basic theorems about Sobolev spaces.

In some applications in \mathbf{R}^3 , it is very helpful to use the special family of radiating solutions to the Helmholtz equation given by

$$e_{l,m}(x) = h_l^{(1)}(kr)Y_{l,m}(\sigma),$$

where $h_l^{(1)}$ is the spherical Hankel function of the first kind and $Y_{l,m}$ are spherical harmonics orthonormal in $L^2(S^2)$ on the unit sphere S^2 . We set out to approximate solutions u to the Helmholtz equation by linear combinations of the form

$$u_\varepsilon(x) = \sum u_{l,m} e_{l,m}(x), \quad m = 0, \dots, 2l+1, \quad l = 0, \dots, N. \quad (9)$$

The following lemma demonstrates that such approximation is indeed possible.

Lemma 4.1 *Let $0 \in \Omega$ and $u \in H_{(1)}(B \setminus \bar{\Omega})$ be a radiating solution to the Helmholtz equation. For any positive ε there is u_ε of the form (9) such that*

$$\|u - u_\varepsilon\|_{(1)}(B \setminus \bar{\Omega}) < \varepsilon. \quad (10)$$

This follows from Theorem 4.1 by expanding u_ε into the series in $e_{l,m}$ and approximating by partial sums of this series.

A similar result is valid for interior problems, if one replaces the functions $e_{l,m}$ by the functions $E_{l,m}(x) = j_l(kr)Y_{l,m}(\sigma)$.

We now discuss how to use these results to approximate u by u_ε . Let Ω_* be a subdomain of $B \setminus \Omega$. Setting $\varepsilon = 1$ in (10), we conclude that for $\varepsilon < 1$ there exist approximating functions u_ε such that

$$\|u_\varepsilon\|_{(1)}(\Omega_*) \leq M_1 = \|u\|_{(1)}(B \setminus \bar{\Omega}) + 1. \quad (11)$$

A weaker version of this constraint is

$$\|u_\varepsilon\|_{(0)}(\Omega_*) < M_0 \leq M_1. \quad (12)$$

Since the data are given on Ω_0 , one can try to approximate u by u_e by solving the minimization problem

$$\min \|u - u_e\|_{(1)}(\Omega_0) \tag{13}$$

subject to the constraint (11) or the weaker constraint (12). Solving this problem for sufficiently large $N = N(\delta)$, one finds $u_e(; \delta)$ such that

$$\|u - u_e(; \delta)\|_{(1)}(\Omega_0) < \delta,$$

and that the constraint (12) holds.

In the following lemma, we denote by $\Omega_{*,d}$ the collection of points of Ω_* which are at distance d from Ω .

Lemma 4.2 *Let Ω_0 be a bounded domain and $\bar{\Omega}_0 \subset \Omega_+$.*

Then there are positive constants C and $\lambda < 1$ depending on Γ, Ω_, d and k , such that*

$$\|u - u_e\|_{(0)}(\Omega_{*,d}) \leq C (\delta + \|u\|_{(1)}(B \setminus \Omega)^{1-\lambda} \delta^\lambda).$$

In addition, if $\Omega_ \subset \text{conv}(\Omega_0)$, the convex hull of Ω_0 , then there are constants C and $\lambda < 1$ depending on Γ, Ω_* and d , such that*

$$\|u - u_e\|_{(1)}(\Omega_{*,d}) \leq C \left(\delta + \frac{\|u\|_{(1)}(B \setminus \Omega)^{1-\lambda} \delta^\lambda}{1+k} \right).$$

This lemma follows from known stability estimates in the Cauchy problem for elliptic equations [I] and from Theorem 2.2.

5 Numerical results.

We give two examples of numerical calculations illustrating our theoretical results. In Example 1, we illustrate the effectiveness of the single layer approach combined with the CGNE (Conjugate Gradient for Normal Equations) stopping rule on a three dimensional problem using actual experimental data taken on Ω , the interior of a cylindrical aircraft fuselage section. In Example 2, we compare the single layer approach with the HELS method in two dimension for a problem on the exterior of a disk where data are taken and recovered locally on arcs.

We solve the discretized equation (3) for a range of wave numbers k . Recall that $k = \omega/c$, where ω denotes the frequency and c is the speed of sound. In the case of the interior aircraft and the range of interest of k is $0.06\pi < k < 3\pi$.

Example 1. This example uses data taken on a cylindrical test section (Γ) from a Cessna business jet at the U. S. Naval Research Laboratory. A 64×32 array of microphone measurements is taken on a concentric cylindrical surface (Γ_0) in the nearfield. The (exact) velocity on Γ was also measured. The pressure data is Fourier analyzed into over

1000 frequencies. We only analyze two frequencies, $98.9MHz$ in Figure 1 and $164.8MHz$ in Figure 2 corresponding to $k \approx 1.8/m$ and $k \approx 3.0/m$, respectively. We use single layer alone, to demonstrate the effectiveness of the combination of our new stopping rule with the single layer representation to reconstruct the velocity on the fuselage.

The upper left hand frame in Figures 1 and 2 displays the exact velocity. The x -axis of the plot is parallel to the center axis of the cylinder and the y -axis is parallel to the circumference. The upper right hand plot is the stopping rule ψ_i (solid line) with the minimum circled. Often a local minimum gives a good choice for the optimal solution. The dashed line is the norm of the difference between successive iterates i of the density $\|\varphi_{i+1} - \varphi_i\|$. When these successive variations have settled down, it provides an indication that the optimal regularized solution has been reached. It is useful, in practice, to have more than one method to choose the regularization parameter.) The remaining four frames in the Figures display the reconstructed velocity at the indicated CGNE iterates. The optimal solution is displayed. Note that it captures many of the features of the exact velocity. The early iterates are overregularized (oversmoothed) and the latter iterates become underregularized (undersmoothed) and exhibit the effects of amplified measurement errors. The matrices S and K are 1282×1282 and it takes about 2 seconds per CGNE iteration to produce the velocity plots. One can therefore easily watch the successive iterates “tune” to the optimal solution. The BEM construction of the matrices S and K . The SVD of the full matrix S for the TSVD take about 20 minutes each on a 950 MHz PC.

We note that only about every second NRL circumferential data point was used in our computations (hence, the different scales on the y -axes of the displays), so that our higher frequency calculation may be somewhat underresolved. In addition, the endcap data may have been slightly misaligned. Nevertheless, the reconstructions are quite reasonable. The bright “hotspots” are at the window locations. We plan more extensive tests on laboratory data in the future.

Example 2. In this example we describe our numerical experiments devoted to the reconstruction of the normal velocity along a curve from the acoustical pressure in two dimensions. We consider three concentric arcs Γ , Γ_{01} and Γ_{02} defined as follows:

$$\Gamma = \{x : \|x\| = r_0, \theta_1 < \arg(x) < \theta_2\}, \quad (14)$$

$$\Gamma_{01} = \{x : \|x\| = r_1, \phi_1 < \arg(x) < \phi_2\}, \Gamma_{02} = \{x : \|x\| = r_2, \phi_1 < \arg(x) < \phi_2\}. \quad (15)$$

We attempt to recover the outward normal velocity $v = \partial_\nu u$ on arc Γ from the acoustic pressure measurements u on arcs Γ_{01} and Γ_{02} . We employ two methods: one based on a single layer representation of the potential, and the HELS method proposed by Sean Wu, see [Wu].

The charge density φ is computed from the pressures $u(x)$ on arcs Γ_{01} and Γ_{02} , and then the normal velocity on arc Γ is found from the formula (4). The operator K used above is defined as the second term in (4).

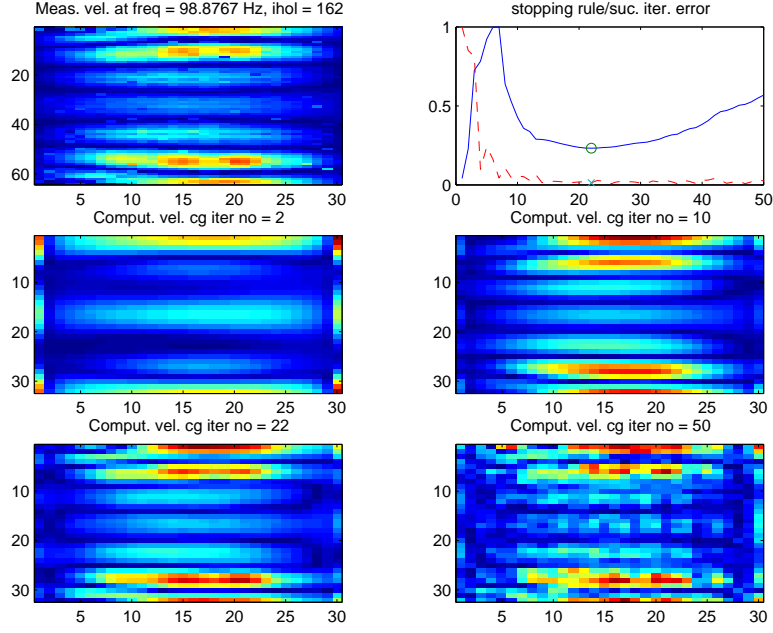


Figure 1: Iterative reconstruction for the cylindrical test section at the US Naval Research Laboratory: lower frequency.

We perturb the exact pressures u by adding noise of the relative intensity $\delta > 0$. Our simulated measurements are thus $u^\delta = u + \xi$, where ξ is a random vector with $\|\xi\|_2 = \delta\|u\|_2$. The system $S_n\varphi = u^\delta$ is solved using the Conjugate Gradient on the Normal Equations (CGNE). For each $m = 1, 2, \dots$, we obtain a regularized charge density φ_m . Then we create a sequence of approximate normal velocities $v_N = K_N\varphi_N$. We choose the iteration number m_0 to minimize the relative L^2 error of the normal velocities

$$\text{err}_m = \frac{\|v - v_m\|_2}{\|v\|_2}.$$

We denote the minimal error by err_0 :

$$\text{err}_0 = \min_m \text{err}_m. \quad (16)$$

Experiment 1. We first consider arcs Γ_{01} and Γ_{02} , respectively, described by equations (15) with parameters $\phi_1 = \frac{7\pi}{8}$, $\phi_2 = \frac{9\pi}{8}$, $r_1 = 1.05$, and $r_2 = 1.10$. Arc Γ is given by (14) with parameters $r = 1$, $\theta_1 = \frac{i\pi}{8}$, $\theta_2 = \frac{9\pi}{8}$. We place acoustic charges with strengths w_1, w_2, \dots, w_p at the points x_1, x_2, \dots, x_p , and thus the resulting pressure u is given by

$$u(x) = \sum_{i=1}^p w_i \Phi(x, x_i).$$

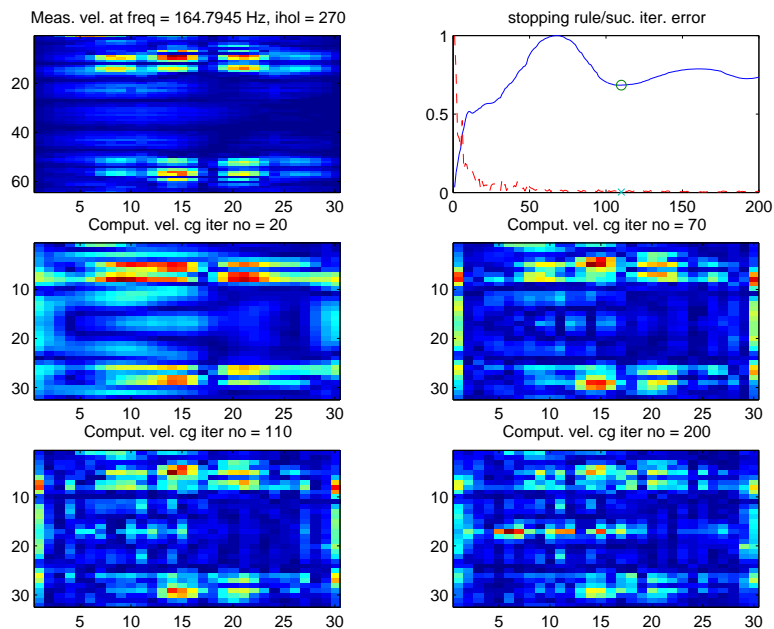


Figure 2: Iterative reconstruction for the cylindrical test section at the US Naval Research Laboratory: higher frequency.

We use $p = 5$ charges with strengths and locations given in Table 1. The pressures are perturbed with noise of the relative intensity $\delta = 0.01$.

Table 2 presents the minimal relative errors of the normal velocities v_m as defined in (16) for wave numbers $k = 1, 3, 6, 12$. The second column of the table contains err_0^1 , the minimal error corresponding to the wave numbers in the first column when $\phi_1 = \frac{7\pi}{8}$, $\phi_2 = \frac{9\pi}{8}$. The last column contains the relative error err_0^2 when $\phi_1 = \frac{3\pi}{4}$, $\phi_2 = \frac{5\pi}{4}$. Each relative error err_0^1 and err_0^2 is the average over 20 trials.

Experiment 2. We solve the same problems using the HELS method. We approximate the potential with $n = 15$ radial wave functions centered at the origin. The normal velocities are approximated by formally differentiating the basis functions. The relative

1.0	(-0.73910, 0.30615)
4.0	(-0.78463, 0.15607)
5.0	(-0.80000, 0.00000)
2.0	(-0.78463, -0.15607)
3.0	(-0.73910, -0.30615)

Table 1: The strengths and locations of the acoustic charges.

k	err ₀ ¹	err ₀ ²
1.0	0.084	0.026
3.0	0.065	0.011
6.0	0.036	0.011
12.0	0.029	0.004

Table 2: Relative errors of the normal velocities for the single layer method.

k	err ₀ ¹	err ₀ ²
1.0	0.024	0.017
3.0	0.011	0.014
6.0	0.010	0.005
12.0	0.025	0.008

Table 3: Relative errors of the normal velocities for the HELS method.

errors are presented in Table 3. As before, the errors are averaged over 20 trials.

We observe immediately that for the layer method, the reconstruction of the normal velocities improves as the wave number k increases. When the HELS method is used, the relative errors are very close to the noise level for all wave numbers considered, so increased stability is visible to a limited extent. In both cases $\text{err}_0^1 > \text{err}_0^2$, which only shows that a better reconstruction is possible with more measurement data.

Acknowledgements. This research was in part supported by the NSF ITR/ACS grant 0081270. We thank Earl Williams, Brian Houston, and Pete Hedric of the NRL Physical Acoustics Group for use of the data taken on the Cessna test section in Example 2 and Lianju Wang for help with the MATLAB code for processing the data.

References

- [DIVW1] T. DeLillo, V. Isakov, N. Valdivia, and L. Wang, *The Detection of the Source of Acoustical Noise in Two Dimensions*, SIAM Journal of Applied Math. , **61** (2001), 2104-2121.
- [DIVW2] T. DeLillo, V. Isakov, N. Valdivia, L. Wang, *The detection of surface vibrations from interior acoustical pressure*, Inverse Problems, **19** (2003), 507–524.
- [HI] T. Hrycak, V. Isakov, *Increased stability in the continuation of solutions to the Helmholtz equation*, Inverse Problems, **20** (2004) (to appear).

- [I] V. Isakov, *Inverse Problems for Partial Differential Equations*, Springer-Verlag, New York, 1998.
- [IW] V. Isakov, S. Wu, *On theory and application of the Helmholtz equation least squares method in inverse acoustics*, *Inverse Problems*, **18** (2002), 1147-1159.
- [J] F. John, *Continuous dependence on data for solutions of partial differential equations with a prescribed bound*, *Comm. Pure Appl. Math.*, **13** (1960), 551-585.
- [W] E. G. Williams, *Fourier Acoustics*, Academic, New York, 1999.
- [Wu] S. Wu, *Nearfield acoustic holography and its evolution*, submitted for publication.